Hard-x-ray spectrographs with resolution beyond 100 μeV

Yuri Shvyd'ko,[1,*] Stanislav Stoupin,[1] Kiran Mundboth,[2] and Jungho Kim[1]
[1]*Advanced Photon Source, Argonne National Laboratory, Argonne, Illinois 60439, USA*
[2]*Diamond Light Source Ltd, Didcot Oxfordshire OX11 0DE, United Kingdom*
(Received 15 October 2012; published 25 April 2013)

Spectrographs take snapshots of photon spectra with array detectors by dispersing photons of different energies into distinct directions and spatial locations. Spectrographs require optics with a large angular dispersion rate as the key component. In visible light optics, diffraction gratings are used for this purpose. In the hard-x-ray regime, achieving large dispersion rates is a challenge. Here we show that multicrystal, multi-Bragg-reflection arrangements feature cumulative angular dispersion rates almost two orders of magnitude larger than those attainable with a single-Bragg reflection. As a result, the multicrystal arrangements become potential dispersing elements of hard-x-ray spectrographs. The hard-x-ray spectrograph principles are demonstrated by imaging a spectrum of photons with a record high resolution of $\Delta E \simeq 90$ μeV in the hard-x-ray regime, using multicrystal optics as the dispersing element. The spectrographs can boost research using inelastic ultrahigh-resolution x-ray spectroscopies with synchrotrons and seeded x-ray free electron lasers.

DOI: 10.1103/PhysRevA.87.043835 PACS number(s): 42.25.−p, 07.85.Nc, 41.50.+h, 61.05.cp

I. INTRODUCTION

A dream x-ray spectrometer is actually a spectrograph that images x-ray spectra in a single shot, with required spectral resolution. State-of-the-art single-shot x-ray spectrometers [1–4] are imaging spectra with array detectors, using Bragg diffraction of x rays from a crystal. Bragg's law dispersion underlies the principles of operations, which links the angle of incidence θ to the energy E of photons Bragg-reflected from the crystal atomic planes. The spectral resolution of the Bragg's law dispersion spectrometers is, however, always limited by the Bragg reflection (Darwin) bandwidth.

Angular dispersion is one way to overcome the Darwin width limitation and substantially improve spectral resolution of x-ray optics [5,6]. Angular dispersion is a variation of the photon angle of reflection θ', with photon energy E, for a fixed incidence angle θ. Angular dispersion takes place in Bragg diffraction, albeit only if the diffracting atomic planes are at a nonzero angle $\eta \neq 0$ (asymmetry angle) to the entrance crystal surface [5,7,8]; see Fig. 1(b). Unlike Bragg's law dispersion, angular dispersion links θ' to E for a fixed θ. Angular dispersion is independent of the Darwin width, and can be therefore used to resolve much narrower spectral features [9]. Because of the principle difference between Bragg's law dispersion and angular dispersion, new concepts are required, to realize single-shot angular dispersive spectrographs.

We introduce here an angular dispersive x-ray spectrograph of a Czerny-Turnertype [10]. Czerny-Turner grating spectrographs are nowadays standard in infrared, visible, and ultraviolet spectroscopies [11,12]. In its classical arrangement, the spectrographs comprise, first, a collimating mirror M_C, which collects photons from a radiation source S and collimates the photon beam [see Fig. 1(a)]; second, an angular-dispersive element DE such as a diffraction grating or a prism, which disperses photons of different energies into different directions; third, a curved mirror M_F which focuses photons of different energies onto different locations $x(E)$, and, last but not least, a spatially sensitive detector Det placed in the focal plane to record the whole photon spectrum. To achieve high resolution, the most important factor is the magnitude of the angular dispersion rate $\mathcal{D} = \delta\theta'/\delta E$, which measures the variation of the reflection angle θ' with photon energy E upon reflection from the dispersing element. For the given mirror focal length $\mathcal{F}$, $\mathcal{D}$ determines the variation of the source image position $x(E)$ on the detector with respect to photon energy: $\delta x(E) = \mathcal{D}\mathcal{F}\,\delta E$. The smallest spectral interval ΔE that can be resolved is, therefore,

$$\Delta E = \frac{1}{\mathcal{D}}\frac{\Delta x}{\mathcal{F}}, \tag{1}$$

where Δx is the largest of either the source S image size or the detector spatial resolution.

Nowadays, diffraction grating manufacturing technology has advanced to the extent that grating spectrographs are being successfully used with much shorter wavelengths, in particular, in the soft x-ray regime ($\lesssim$1 keV) [13] attaining resolving power of $E/\Delta E \simeq 10^4$. Extension into the hard-x-ray regime is, however, not trivial, because of the lack of hard-x-ray optics elements with a sufficiently large dispersion rates.

A hard-x-ray equivalent of the diffraction grating is a Bragg diffracting crystal with diffracting atomic planes at an asymmetry angle $\eta \neq 0$ to the entrance crystal surface [Fig. 1(b)] [5,7,8]. The use of asymmetrically cut crystal as the dispersing element in combination with a single focusing element was proposed for a "focusing monochromator" [14]. However, as the authors of [14] correctly mentioned, such an arrangement can be used as a monochromator, however, not as a spectral analyzer (or spectrograph), as a small angular size of the radiation source is required for its realization.

Angular dispersion rates attained in a single Bragg reflection are typically small $\mathcal{D} \simeq 8$ μrad/meV [6,9], and are the main obstacle in realization of hard-x-ray spectrographs. In Sec. II we show that the angular dispersion rate can be enhanced dramatically, by successive asymmetric Bragg reflections, by almost two orders of magnitude compared to that in a single Bragg reflection. In Sec. III we demonstrate

*shvydko@aps.anl.gov

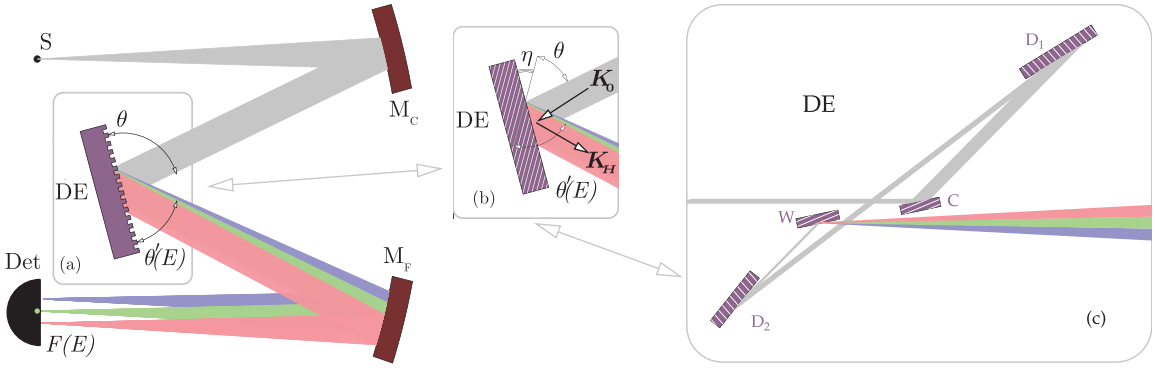

FIG. 1. (Color online) Scheme of the Czerny-Turner-type [10] spectrograph with a diffraction grating (a), or a crystal in asymmetric x-ray Bragg diffraction (b) as a dispersing element, DE. Other components include radiation source S, collimating and focusing mirrors M_C and M_F, and position-sensitive detector Det. (c) Multicrystal multireflection CDFDW optics [9] is an example of a hard-x-ray "diffraction grating" (DE element) with an enhanced dispersion rate, suitable for hard-x-ray spectrographs.

this effect on an example of the so-called CDFDW multicrystal optics [20], by measuring a cumulative dispersion rate of $\mathcal{D}_{\rm CDFDW} = 314$ μrad/meV. As a result, the multicrystal arrangements become potential dispersing elements of hard-x-ray spectrographs. A prototype hard-x-ray spectrograph with the multicrystal, multireflection CDFDW optics as the dispersing element is demonstrated in Sec. IV, by imaging an x-ray spectrum of 9.1315-keV photons in a 450-μeV window with a record small 90-μeV resolution, thus achieving spectral resolution power beyond 10^8 in the hard-x-ray regime.

II. ANGULAR DISPERSION RATE ENHANCEMENT—THEORY

Let $\boldsymbol{K}_0$ be the momentum of the incident x-ray photon, and $\boldsymbol{K}_H$ be the momentum of the photon reflected from a crystal in Bragg reflection with the diffraction vector $\boldsymbol{H}$. The vectors $\boldsymbol{K}_0$ and $\boldsymbol{K}_H$ make angles $\theta+\eta$, and $\theta'-\eta$, respectively, with the crystal surface [Fig. 1(b)]. Here θ and θ' are the glancing angles of incidence and reflection with respect to the diffracting atomic planes, and η is an asymmetry angle between the crystal surface and the diffracting atomic planes. The asymmetry angle η is defined here to be positive in the geometry shown in Fig. 1(b), and negative in the geometry with reversed incident and reflected x rays (not shown).

Conservation of the tangential components $(\boldsymbol{K}_H)_t = (\boldsymbol{K}_0 + \boldsymbol{H})_t$ with respect to the entrance crystal surface, and the conservation of the photon energies $|\boldsymbol{K}_H|\hbar c = |\boldsymbol{K}_0|\hbar c = K\hbar c = E$ require that [15]

$$\cos(\theta'-\eta) = \cos(\theta+\eta) + \frac{H}{K}\sin\eta. \tag{2}$$

Differentiating over E, using Bragg's law $2K\sin\theta = H$, and assuming $|\theta'-\theta| \ll 1$, we obtain

$$\frac{d\theta'}{dE} = -b\frac{d\theta}{dE} + \mathcal{D}, \tag{3}$$

$$\mathcal{D} = \frac{2\sin\theta\sin\eta}{E\sin(\theta-\eta)}. \tag{4}$$

Here

$$b = -\frac{\sin(\theta+\eta)}{\sin(\theta-\eta)} \tag{5}$$

is the asymmetry ratio. If the incident beam is collimated, $d\theta/dE = 0$, then $d\theta'/dE = \mathcal{D}$, where $\mathcal{D}$ (4) is an intrinsic angular dispersion rate upon single Bragg reflection [5,7]. If, however, the incident x rays are dispersed, $d\theta/dE \neq 0$, then the dispersion rate $d\theta'/dE = \mathcal{D}_{\rm out}$ becomes

$$\mathcal{D}_{\rm out} = b\mathcal{D}_{\rm in} + \mathcal{D}, \tag{6}$$

where $\mathcal{D}_{\rm in} = -d\theta/dE$ is the angular dispersion rate of the incident x rays. The minus sign follows the convention that the counterclockwise sense of angular variations in θ and θ' is positive. Similarly, if the sense of deflection of the ray upon the Bragg reflection is clockwise, unlike that shown in Fig. 1(b) the counterclockwise case, the single crystal intrinsic dispersion rate $\mathcal{D}$ in Eq. (4) has to be used with sign minus.

Equation (6) demonstrates that the angular dispersion rate $\mathcal{D}_{\rm in}$ can be indeed significantly enhanced by a successive asymmetric Bragg reflection, if its asymmetry ratio is large: $|b| \gg 1$. The enhancement can be even larger if several $(1,2,..,n)$ successive reflections are used:

$$\begin{aligned}\mathcal{D}_{\cup_n} &= b_n\mathcal{D}_{\cup_{n-1}} + \mathcal{D}_n \\ &= b_n\{b_{n-1}\ldots[b_3(b_2\mathcal{D}_1+\mathcal{D}_2)+\mathcal{D}_3]\ldots\mathcal{D}_{n-1}\}+\mathcal{D}_n.\end{aligned} \tag{7}$$

III. ANGULAR DISPERSION RATE ENHANCEMENT—EXPERIMENT

In the experiment presented in this section, we demonstrate the effect of the angular dispersion enhancement on an example of a four-crystal angular dispersive CDFDW optics [9], with schematic shown in Fig. 1(c). We use the CDFDW optics to demonstrate essentially new physics of angular dispersion enhancement, which has been disregarded and not used in previous studies [6,9]. In the second proof of the principle experiment presented in Sec. IV, we apply such optics as the "diffraction grating" of a prototype hard-x-ray spectrograph to image a spectrum of the CDFDW with record high spectral resolution. The experiments were performed at the 30ID beamline of the Advanced Photon Source.

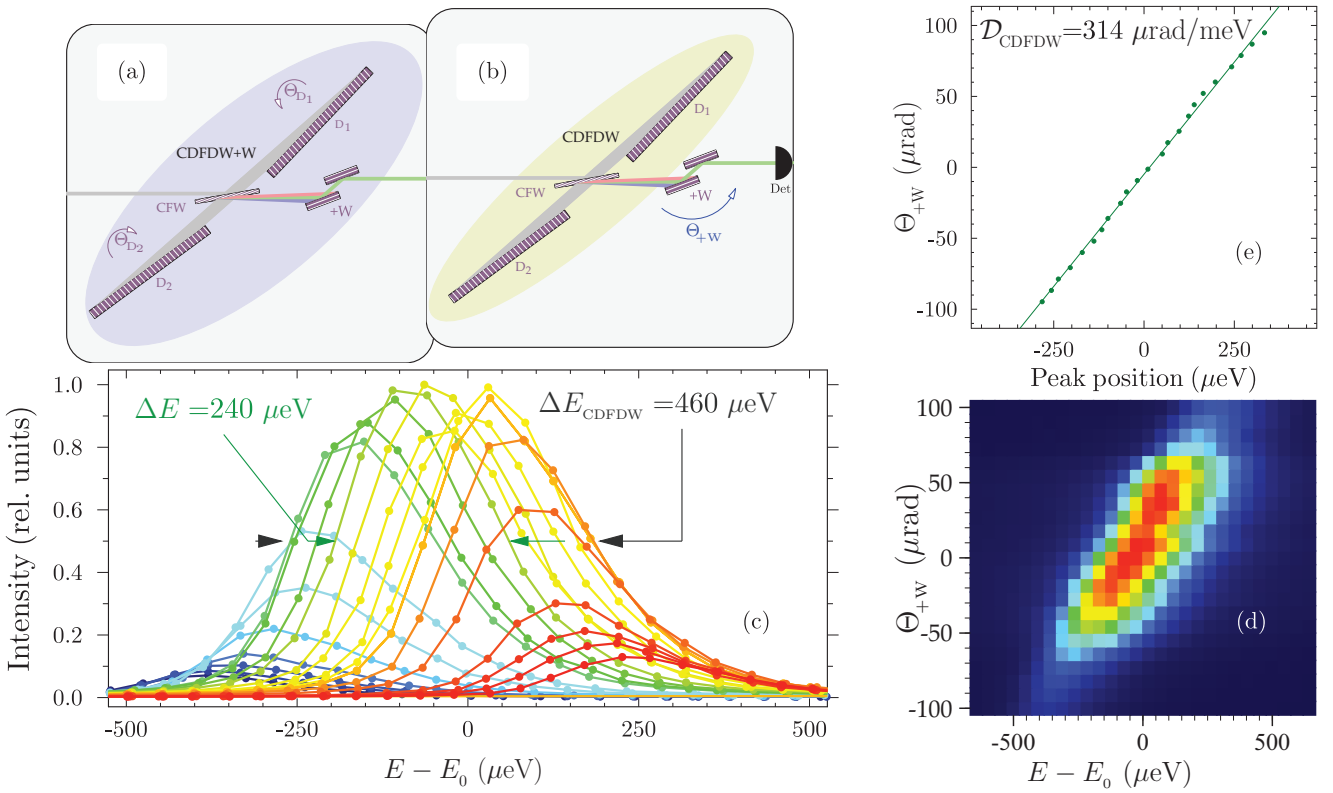

FIG. 2. (Color online) Enhanced angular dispersion rate of the CDFDW optics. Schematic of the experiment showing the CDFDW + W monochromator (a) probing the angular dispersion rate of the CDFDW optics (b) with the + W channel-cut crystal as an angular analyzer. (c) Spectral dependencies of x-ray transmission through the CDFDW optics for fixed angular positions Θ_{+W} of + W. (d) Same as (c) presented as a two-dimensional (2D) plot. (e) Transmission peak position as a function of Θ_{+W}.

A. CDFDW optics as diffraction grating with enhanced angular dispersion rate

Details on the multicrystal CDFDW optics used in this paper are provided in [9]. CDFDW is a modification of the CDW [5,6] optics originally designed to achieve the very high monochromatization of x rays. Importantly, unlike [6,9], the CDFDW optics is used here not as a monochromator. It is used in a different function, as a diffraction grating with a greatly enhanced angular dispersion rate.

The first element—C (collimator)—is a Si asymmetrically cut crystal, with the 220 Bragg reflection, $\theta_C = 20.7°$, $\eta_C = 19.0°$, $b_C = -1/21.5$, accepting x rays with photon energy $E = 9.1315$ keV in a wide angular range $\simeq$110 μrad, and collimating it to a beam with a factor $|b_C|$ smaller divergence $\simeq$5 μrad, and negligible $\mathcal{D}_C = 0.040$ μrad/meV.

The next two Si crystals—D_1 and D_2—are designed to produce a maximal intrinsic single crystal Bragg dispersion rate $\mathcal{D}$ (4), using the 008 reflection with $\theta_{D_i} \simeq 90°$, $\eta_{C_i} = 88.0°$, $b_{D_i} \simeq -1$ $(i = 1,2)$, and $\mathcal{D}_{D_1} = -\mathcal{D}_{D_2} = 6.27$ μrad/meV. We would like to note, that the scheme in Fig. 1(c) is shown in a universal configuration with $\theta_{D_i} \neq 90°$, to emphasize that in general it is not restricted to the one used in the experiment particular case of $\theta_{D_i} \simeq 90°$. Shown in Fig. 1(c) the universal CDFDW scheme is a straightforward generalization of the universal CDW scheme presented in [5], obtained by adding the second D crystal [21].

The fourth crystal W is equivalent to the C crystal, however, applied in an inverse configuration with $\eta_W = -\eta_C$, $b_W = 1/b_C = -21.5$, and $\mathcal{D}_W = 0.86$. It is used to enhance the angular dispersion rate of the D crystals. Indeed, applying Eq. (7) we estimate the cumulative dispersion rate of the optics: $\mathcal{D}_\cup \simeq b_W(\mathcal{D}_{D_2} - \mathcal{D}_{D_1}) + \mathcal{D}_W \simeq 2b_W\mathcal{D}_{D_1} \simeq -270$ μrad/meV, enhanced by a factor $2|b_W| \simeq 43$ compared to the dispersion rate achieved in a single Bragg reflection. The same enhancement factor was derived in [16,17] using DuMond diagram analysis.

Figure 2 shows a schematic of the first experiment and results of measurements of the angular dispersion rate of the CDFDW optics. A tunable monochromator CDFDW + W with an $\simeq$170-μeV bandwidth shown schematically in Fig. 2(a), and described in detail in Sec. III B, is used to measure transmission spectra through the CDFDW optics under study [presented in Fig. 2(b)]. An auxiliary element denoted as + W in Fig. 2(b) is used to extract from all x-ray photons emanating from the CDFDW optics a small part with $\simeq 20 - \mu$rad divergence by the 220 symmetric Bragg reflection from a Si channel-cut crystal (angular acceptance 20 μrad). For each angular position Θ_{+W} of the + W crystal, a spectrum of x rays transmitted through the CDFDW optics and through the + W angular analyzer is measured, as shown in Fig. 2(c). Figure 2(d) presents a 2D plot of the spectra. The peak of the spectral distribution changes with the emission angle defined

by Θ_{+W}. Figure 2(e) shows that the dependence is linear, with the tangent $\mathcal{D}_{CDFDW} = 314$ μrad/meV representing the measured cumulative dispersion rate of the CDFDW optics. The number is $\simeq$15% larger than the estimated one, which we attribute to the difference between the nominal and real asymmetry angles. This result confirms the theoretical prediction, expressed by Eqs. (6) and (7), that the angular dispersion rate can be substantially enhanced in multicrystal arrangements.

B. CDFDW + W monochromator

A few details regarding the monochromator in Fig. 2(a) are in order: It is the same CDFDW optics, however, enhanced with the +W channel cut that substantially decreases the CDFDW bandwidth. The energy tuning of the CDFDW + W monochromator is performed by synchronous change of the angular orientation of the D crystals, as indicated by Θ_{D_i} in Fig. 2(a), and explained in more detail in [9]. Each spectral dependence in Fig. 2(c) has a width of $\Delta E \simeq 240 \pm 12$ μeV. This number represents the width of the convolution of the spectral distributions of the CDFDW + W monochromator [Fig. 2(a)], and the analyzer [Fig. 2(b)]. Assuming they are equivalent, the spectral width of a single CDFDW + W optics is estimated as $\Delta E/\sqrt{2} \simeq 170 \pm 9$ μeV. The theory [16,17] predicts a smaller bandwidth of 100 μeV.

An envelope of spectral dependencies in Fig. 2(c) reveals a total width of $\Delta E_{CDFDW} \simeq 460 \pm 23$ μeV of the CDFDW optics. A similar number has been measured in [9], which is also broader than predicted in theory $\simeq 400$ μeV. The discrepancies are attributed to imperfections of the real crystal optics.

IV. PROTOTYPE X-RAY SPECTROGRAPH

In the second experiment, presented in this section, the CDFDW optics with the greatly enhanced dispersion rate demonstrated above is used as a "diffraction grating" of a prototype hard-x-ray spectrograph. Figure 3(a) shows the proof-of-principle spectrograph setup, in which the CDFDW optics is augmented with a focusing mirror M_F and a position sensitive detector placed at the mirror focal distance $\mathcal{F} = 1.38$ m. The polychromatic collimated beam, which in a complete spectrograph setup would be created by the collimating mirror M_C, as in Fig. 1(a), is mimicked here by the incident x-ray beam with a $\lesssim$15-μrad angular divergence and a bandwidth of $\simeq$0.6 eV. This beam directly focused by mirror M_F has a $\simeq$30-μm spot size.

Figure 3(b) shows the spatial distribution of x rays transmitted through the CDFDW optics and imaged on the detector with mirror M_F. It is $\simeq$160-μm broad, i.e., much broader than the $\simeq$30-μm image size of the incident beam, and has a double peak structure. We believe that this distribution presents the image of the spectrum of x rays transmitted through the CDFDW optics. It is relevant to the spectral dependencies shown in Fig. 2(c), however, with a more pronounced minimum near $x = 0$, as no convolution with the monochromator spectral function is involved. The spatial width $\Delta x \simeq 160$ μm corresponds to the spectral width, which we know should be $\simeq$450 μeV. The results shown in Fig. 4(b),

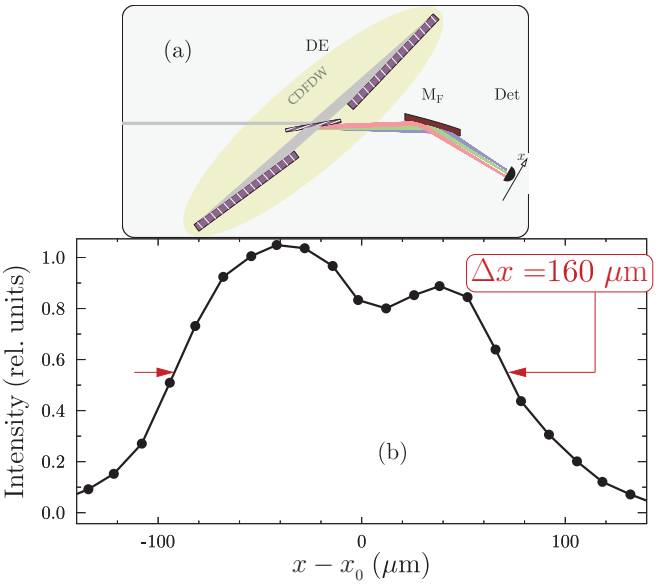

FIG. 3. (Color online) Image of the CDFDW spectral function on the spatial x scale (b) measured in the prototype spectrograph setup (a).

which were measured in a modified experimental scheme presented in Fig. 4(a), confirm this.

The experimental scheme in Fig. 4(a) is complemented by the +W channel cut which, as we know from the results presented in Fig. 2, selects an x ray emanating in a certain direction from the CDFDW optics, and, as a result, within a reduced bandwidth, whose central photon energy is defined by the angle Θ_{+W}. Figure 4(b) shows the spatial distribution of x rays measured at different Θ_{+W} values. The peak positions, plotted in Fig. 4(d), change in the first approximation linearly with Θ_{+W} at a rate $\mathcal{D}_F = 1.13$ μm/μrad. Together with the results presented in Fig. 2(e) this proves that the spectral distribution of x rays from the CDFDW optics is imaged by mirror M_F on the spatial scale, with a conversion factor $\mathcal{D}_F\mathcal{D}_{CDFDW} \simeq 355$ μm/meV. Using this number, we obtain that the total widths of the spatial distributions in Figs. 3(b) and 4(b) are $\Delta E_{CDFDW} \simeq 450 \pm 20$ μeV, representing the spectral width of the CDFDW optics.

The spatial widths of single lines vary from 32 μm (in green) to 50 μm (in yellow), corresponding to spectral widths $\simeq 90 \pm 5$ μeV and $\simeq 140 \pm 7$ μeV, respectively. The resolution of the CDFDW spectrograph is at least $\simeq$90 μeV. In fact it is even better, limited in the present experiment by the focal spot size, and the bandwidth of the photons singled out by the +W channel cut.

The fact that the widths of the single lines vary across the CDFDW spectrum, as well as the fact that the CDFDW spectrum has a double-peak structure, imply that the CDFDW optics we have built is not yet perfect. This is consistent with the results of [9], where a somewhat broader line was measured as expected from theory. However, now using the CDFDW in the spectrograph setup, we can measure and analyze the CDFDW spectrum directly, without the need of another CDFDW optics as an analyzer. Using Eq. (1) with $\mathcal{F} = 1.38$ m, $\Delta x = 32$ μm, and the theoretically estimated

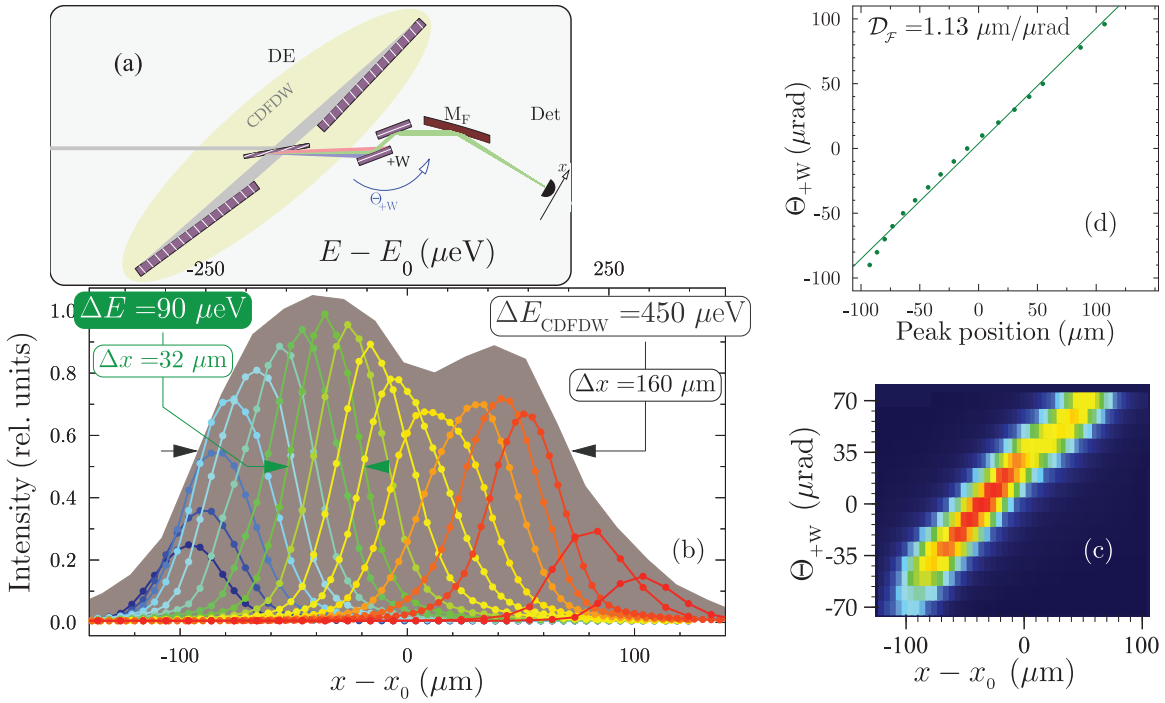

FIG. 4. (Color online) Prototype hard-x-ray spectrograph with a ≃90-μeV resolution using CDFDW optics as dispersing element (DE). (a) Schematic of the experiment. (b) Images of the CDFDW + W spectral function on the spatial x scale for fixed angular positions Θ_{+W} of + W. The gray profile in the background is the image of the CDFDW spectral function from Fig. 3(b). (c) Same as (b) presented as a 2D plot. (d) Spatial peak position as a function of Θ_{+W}.

$\mathcal{D}_\cup = 270$ μrad/meV, we obtain $\Delta E = 86$ μeV in agreement with the measured energy resolution.

V. CONCLUSIONS

In conclusion, a principle is proposed and demonstrated on how to enhance by almost two orders of magnitude the angular dispersion rate of x rays in Bragg diffraction, namely by successive asymmetric Bragg reflections. This effect opens an opportunity of realizing dispersing elements in the hard-x-ray regime with an angular dispersion rate sufficiently large for practical use in x-ray spectrographs. The hard-x-ray spectrograph principle is demonstrated with the multicrystal, multireflection CDFDW optics as the dispersing element, by imaging an x-ray spectrum of 9.1315-keV photons in a 450-μeV window with a record small 90-μeV resolution, thus achieving spectral resolution power beyond 10^8 in the hard-x-ray regime.

The main future effort should be directed not only to further improving the spectral resolution, but primarily into making the spectral window broader, to enhance the spectrographs throughput.

Hard-x-ray spectrographs can advance significantly research using high-resolution x-ray spectroscopies, in particular different branches of inelastic x-ray scattering, at synchrotrons and seeded XFELs [18].

ACKNOWLEDGMENTS

We are grateful to L. Young for supporting this project at the Advanced Photon Source (APS), and to S. Collins and G. Materlik at the Diamond Light Source (DLS). D. Shu, T. Roberts, K. Goetze, J. Kirchman, P. Jemian, M. Upton, and Y. Ding are acknowledged for technical support. Work was supported by the US Department of Energy, Office of Science, Office of Basic Energy Sciences, under Contract No. DE-AC02-06CH11357.

[1] T. Matsushita and R. P. Phizackerley, Jpn. J. Appl. Phys. **20**, 2223 (1981).
[2] S. Huotari, G. Vanko, F. Albergamo, C. Ponchut, H. Graafsma, C. Henriquet, R. Verbeni, and G. Monaco, J. Synchrotron Radiat. **12**, 467 (2005).
[3] M. Yabashi, J. B. Hastings, M. S. Zolotorev, H. Mimura, H. Yumoto, S. Matsuyama, K. Yamauchi, and T. Ishikawa, Phys. Rev. Lett. **97**, 084802 (2006).
[4] D. Zhu, M. Cammarata, J. M. Feldkamp, D. M. Fritz, J. B. Hastings, S. Lee, H. T. Lemke, A. Robert, J. L. Turner, and Y. Feng, Appl. Phys. Lett. **101**, 034103 (2012).
[5] Yu. Shvyd'ko, *X-Ray Optics—High-Energy-Resolution Applications*, Vol. 98 of *Optical Sciences* (Springer, Berlin/Heidelberg/New York, 2004).
[6] Yu. V. Shvyd'ko, M. Lerche, U. Kuetgens, H. D. Rüter, A. Alatas, and J. Zhao, Phys. Rev. Lett. **97**, 235502 (2006).

[7] T. Matsushita and U. Kaminaga, J. Appl. Crystallogr. **13**, 472 (1980).
[8] S. Brauer, G. Stephenson, and M. Sutton, J. Synchrotron Radiat. **2**, 163 (1995).
[9] Yu. Shvyd'ko, S. Stoupin, D. Shu, and R. Khachatryan, Phys. Rev. A **84**, 053823 (2011).
[10] M. Czerny and A. F. Turner, Z. f. Physik **61**, 792 (1930).
[11] A. B. Shafer, L. R. Megill, and L. Droppelman, J. Opt. Soc. Am. **54**, 879 (1964).
[12] K.-S. Lee, K. P. Thompson, and J. P. Rolland, Opt. Express **18**, 23378 (2010).
[13] G. Ghiringhelli, A. Piazzalunga, C. Dallera, G. Trezzi, L. Braicovich, T. Schmitt, V. N. Strocov, R. Betemps, L. Patthey, X. Wang *et al.*, Rev. Sci. Instrum. **77**, 113108 (2006).
[14] V. G. Kohn, A. I. Chumakov, and R. Rüffer, J. Synchrotron Radiat. **16**, 635 (2009).
[15] M. Kuriyama and W. J. Boettinger, Acta Cryst. A **32**, 511 (1976).
[16] Yu. Shvyd'ko, arXiv:1110.6662.
[17] Yu. Shvyd'ko, Proc. SPIE **8502**, 85020J (2012).
[18] J. Amann, W. Berg, V. Blank, F.-J. Decker, Y. Ding, P. Emma, Y. Feng, J. Frisch, D. Fritz, J. Hastings *et al.*, Nature Photonics **6**, 693 (2012).
[19] X.-R. Huang, J. Synchrotron Radiat. **18**, 1 (2011).
[20] CDFDW is an abbreviation for five successive Bragg reflections (from three crystals) in the optics introduced in [9] with each Bragg reflection having a certain key function denoted as C for collimator, D for dispersing element, F for anomalous transmission filter, and W for wavelength selector, respectively.
[21] We note also here that the "alternative scheme" proposed in [19] and shown schematically in Fig. 5(a) of [19] cannot function as an angular dispersive optics, since the second D crystal in the proposed scheme annihilates the angular dispersion produced by the first D crystal.